Fitness-For-Service Assessment for Pressure Equipment in Chemical Plants

Sumitomo Chemical Co., Ltd.
Process & Production Technology Center
Takuyo KAIDA

Fitness-For-Service (FFS) assessments are quantitative engineering evaluations to demonstrate the structural integrity of an in-service component that may contain a flaw or damage. FFS assessment has become popular in the past ten years. One of the reasons why the assessment has become familiar is that some engineering standards have been published. Recently, the engineering standards have evolved to be more international and comprehensive, for example, by the release of a joint American Petroleum Institute (API)/ American Society of Mechanical Engineers (ASME) FFS standard. This paper provides an interpretation of local metal loss assessment procedures based on API/ASME FFS standard and experimental and numerical validation analysis results of FFS assessment.

This paper is translated from R&D Report, "SUMITOMO KAGAKU", vol. 2009-I.

Introduction

Sumitomo Chemical possesses a large number of aging plants that have been in service over 30 years, centered on facilities that were constructed during the period of high growth in the 1970s, and some of the equipment has reached 40 years of age. On the other hand, we are moving forward with new construction projects such as the construction of a large chemical refining and petrochemical plant in Saudi Arabia and expanding a basic chemical product production plant in Singapore. Safe, stable continuation of operations is an important problem for plants that have this kind of varied history and characteristics.

The design and production technology is important for assuring safety in the pressure equipment at plants. The engineering standards that have been turned into performance specifications for design and production of pressure equipment in Japan are determined by the four laws relating to pressure vessels (High Pressure Gas Safety Act, Industrial Health and Safety Act, Electricity Business Act and Gas Business Act). Provisions for the design specifications are established by Japanese Industrial Standards (JIS).[1] These JIS standards are compatible with the Boiler and Pressure Vessel Code[2] of the American Society of Mechanical Engineers (ASME), which is the international design standard for pressure equipment.

Along with design and production, plant maintenance technology is also important. Maintenance technology is formed on the three pillars of inspection, evaluation, and repair and replacement.[3] Inspection is nondestructive inspection technology for detecting defects arising while the equipment is in service. Evaluation is technology for carrying out evaluations as to whether the defects detected during inspections affect the soundness of the equipment from a destructive mechanical point of view. These evaluations are called Fitness for Service (FFS). Repair and replacement are technologies for carrying out repairs and replacements for the defects determined to affect the health of the plant as a result of the fitness for service evaluations. These technologies provide optimal judgment indicators according to the type and history of the equipment, the type of defect and the strength of materials rather than just carrying out indiscriminate maintenance on each piece of pressure equipment. In the field of nuclear power, operations are started with the specifications for the maintenance methods for nuclear power plants already determined by civil standards.[4]

In the field of pressure equipment for chemical plants in Japan, we try to draft and implement stan-

dards for this plant maintenance technology according to the use of equipment. Accordingly, the Fitness For Service Study Group (FFS Study Group) hosted by the Petroleum Association of Japan and the Japan Petrochemical Industry Association which has focused on API 579-1/ASME FFS-1[5] (API/ASME FFS-1 in the following), consisting of maintenance standards drafted jointly with the American Petroleum Institute (API), and has carried out various other activities. The authors have participated in this study group and have been involved in cooperative studies and exchanges of ideas.

In this article, we are aiming at describing the introduction of FFS technology and will deal with the relationship between the design criteria and maintenance criteria for pressure equipment in chemical plants. In addition, we will give an overview of the background of the technology for local metal loss assessments, which are one FFS technology, and introduce the results of simulations using destructive testing and the finite element method (FEM). In addition, we will give an introduction to the status of studies by the FFS Study Group and discuss the outlook for the future.

Design Criteria and Maintenance Criteria

We need to deal with the relationship with design criteria to aim at introducing maintenance criteria that include FFS technology. We can consider "things must be done while production continues" as a typical concept. However, things always incur damage and deteriorate. Maintenance criteria are criteria for having things for which damage and deterioration are essentially unavoidable in a safe and continuous manner. Here, we will discuss the relationship between these two criteria in terms of what kind of concepts assure safety in the design criteria and maintenance criteria for pressure equipment. We will explain specific concepts in local metal loss assessments for maintenance criteria.

1. Design Criteria[6]

The design criteria for pressure equipment are divided into design by rule and design by analysis. With design by rule, failure modes are represented by plastic collapse and large safety factors are established to assure safety for all failure modes. The plastic collapse of pressure equipment is a state where seals yield across the entire cross-section and deformation progresses in a state with no increase in load when a load is applied. Here, the safety factor S is the factor S when the reference strength σ_c is a fixed value and the allowable stress σ_a is limited as follows.

$$\sigma_a = \frac{\sigma_c}{S} \qquad \text{(Eq. 1)}$$

On the other hand, in design by analysis, all failure modes that can occur are envisioned and detailed stress analyses are carried out. Stress limitations and temperature limitations are implemented, and smaller safety factors than those for design by rule can be established. As examples of design by rule and design by analysis, the normative stress and safety factors in the no-creep range for JIS B8265, B8266 and B8267, which are Japanese design standards, are shown in **Fig. 1**. Moreover, σ_{uts} is the tensile strength of the material and σ_{ys} is the yield stress of the material.[1), 7), 8)]

In the design criteria, the safety factor defined in the equation for allowable stress is established based on forecasts for the state of operation and is an empirical value. A large margin must be taken to assure safety for all failure modes, but by introducing the uniform concept of allowable stress, the thickness necessary for pressure equipment can be determined uniquely for the design, and it has the merit of reducing the effort required for analysis.

JIS B8265	$\sigma_a = \min\left[\frac{\sigma_{uts}}{4}, \frac{\sigma_{ys}}{1.5}\right]$	(Design by rule)
JIS B8266	$\sigma_a = \min\left[\frac{\sigma_{uts}}{3}, \frac{\sigma_{ys}}{1.5}\right]$	(Design by analysis)
JIS B8267	$\sigma_a = \min\left[\frac{\sigma_{uts}}{3.5}, \frac{\sigma_{ys}}{1.5}\right]$	(Design by rule)

Fig. 1 Normative stress and design factor

2. Maintenance Criteria

The role of maintenance criteria is confirming whether the predictions at the time of design were correct or not and continuing safe, stable operation. Fracture morphology is specified by collecting actual data, and safety factors are established. Therefore, the design criteria that consider all fracture modes are different from the safety factors for the maintenance criteria. Furthermore, the concept of a "safety factor for the reference strength" itself is reassessed in the maintenance criteria, and a concept of rational safety assur-

ance according to the failure mode, type of damage, etc. is used.

In local metal loss assessments in API/ASME FFS-1, the failure mode is specified to be plastic collapse. The remaining strength factor (*RSF*) is used as an index for evaluating safety assurance.

$$RSF = \frac{P_{DC}}{P_{UC}} \qquad \text{(Eq. 2)}$$

Here, P_{DC} is the plastic collapse load for equipment that has local metal loss, and P_{UC} is the plastic collapse load for sound equipment. For example, $RSF = 0.8$ expresses the fact that 80% of the strength remains in the equipment, or to put it another way, 20% of the strength has been lost. Safety assessments of equipment are carried out as follows by combining *RSF* with a concept of maximum allowable working pressure (*MAWP*).

(1) Determination of t_c

The thickness t_c used in the assessment is calculated using either Eq. 3 or Eq. 4. This t_c expresses the actual thickness of sound parts.

$$t_c = t_{nom} - LOSS - FCA \qquad \text{(Eq. 3)}$$

$$t_c = t_{rd} - FCA \qquad \text{(Eq. 4)}$$

Here, t_{nom} is the nominal thickness, *LOSS* the uniform local metal loss from construction to the time of the assessment, t_{rd} the thickness at a position away from the local loss and *FCA* presumed future corrosion.

(2) Determination of *MAWP*

MAWP is found using the following equation (when the equipment is a cylindrical vessel).

$$MAWP = \frac{\sigma_a E t_c}{R_i + 0.6 t_c} \qquad \text{(Eq. 5)}$$

Here, σ_a is the allowable stress during design, it E the weld joint efficiency and R_i the inside diameter.

The meaning of *MAWP* in API/ASME FFS-1 is the provisional maximum allowable working pressure assuming equipment that has not undergone local metal loss.

(3) Determination of $MAWP_r$

The maximum allowable working pressure for equipment that has undergone local metal loss is defined by the following equations.

$$MAWP_r = MAWP \qquad for\ \ RSF \geq RSF_a \qquad \text{(Eq. 6)}$$

$$MAWP_r = MAWP \frac{RSF}{RSF_a} \qquad for\ \ RSF < RSF_a \qquad \text{(Eq. 7)}$$

Here, RSF_a is the allowable value for *RSF*.

Operation of pressure equipment that has undergone local metal loss is permitted at a pressure of $MAWP_r$ or less by API/ASME FFS-1. In Eq. 6, the same maximum allowable working pressure for sound equipment is set as $MAWP_r$ only when $RSF \geq RSF_a$. In other words, it is thought that there are no problems with safety if a strength of RSF_a remains even if there has been local metal loss. Eq. 7 imputes the drop in strength because of local metal loss to $MAWP_r$ by multiplying the *MAWP* of equipment that has not undergone local metal loss by *RSF* when $RSF < RSF_a$, and by eliminating RSF_a, the permissible loss of strength is added to $MAWP_r$. By reducing $MAWP_r$ even with the metal loss for $RSF < RSF_a$, this assures a safety margin for the plastic collapse load that is the same as $RSF = RSF_a$

In API/ASME FFS-1, RSF_a is a conservative value of 0.9. The significance of this value is a 10% reduction in strength because of local metal loss is allowable in the maintenance criteria. The definition of primary local membrane stress in design criteria is cited as the basis for the 10% in API/ASME FFS-1. JIS B8266, which is compatible with ASME design standards, has the following description.

"The allowable value for primary local membrane stress intensity arising because of the design load is $1.5kS_m$. Local, here, is the case where primary membrane stress intensity that exceeds $1.1S_m$ does not remain in a range of $2.5\sqrt{R_m t_m}$ along the meridian line from an area where the range of primary membrane stress intensity exceeds $1.1S_m$ within $1.0\sqrt{Rt}$ along the meridian line. Here, S_m is the allowable stress for the material (design stress intensity), k is an augmenting factor the allowable stress is multiplied by, R is the normative radius of the part in question (normal distance from the neutral plane to the neutral axis), t is the minimum thickness of the part in question, and R_m and t_m are the average of the normative radius and average of the minimum thickness for the part where the primary local membrane stress intensity exceeds S_m."

Therefore, the range where the membrane stress

exceeds 10% at the local periphery is ignored in the design criteria. RSF_a = 0.9 is described so as to be compatible with design criteria.

Technical Background of Fitness for Service Assessments for Local Metal Loss [9), 10)]

We dealt with the relationship between design criteria and maintenance criteria in the previous section, and explained safety assessment methods for local metal loss in the maintenance criteria. One of the engineering technologies required in local metal loss assessments is the computation of plastic collapse load for pressure equipment that has undergone local metal loss. To understand the technical background of this, we must start thinking in terms of computations of plastic collapse load for sound pressure equipment. Here, we will give an explanation presuming a cylindrical vessel for the shape of the equipment and the load being internal pressure only.

1. Plastic Collapse of a Sound Vessel

We can think of a sound vessel as undergoing plastic collapse when the stress applied to the seals reaches the flow stress. Assuming a thin-walled cylinder, the plastic collapse load P_{UC} is expressed as follows using the flow stress σ_{flow}, inside diameter D_i and nominal thickness t, when an inside diameter reference is considered.

$$P_{UC} = \frac{2_t}{D_i}\,\sigma_{flow} \qquad \text{(Eq. 8)}$$

In addition, there is the equation below, which was proposed by Nadai and which assumes a thick-walled cylinder.

$$P_{UC} = \frac{2}{\sqrt{3}}\,\sigma_{flow}\ln\left(\frac{R_o}{R_i}\right) \qquad \text{(Eq. 9)}$$

Here, R_o is the outside radius, and R_i is the inside radius. Typically, the yield stress σ_{ys} and average value for the tensile strength σ_{uts} $(\sigma_{ys} + \sigma_{uts})/2$ are used for the flow stress, but there have been various proposals to match this with the results of burst tests.

2. Critical Stress of Cylindrical Vessels Having Cracks Penetrating Axially [11)]

The foundation of methods for estimating plastic collapse loads for cylindrical vessels having local metal loss is based on destructive analysis of pressure cylinders having cracks all the way through. The circumferential stress during breaking due to internal pressure on cylinders having cracks that pass through axially is lower than the critical stress for flat plates having cracks that pass through, and cylinders are weaker than flat plates.

This is not only because cylinders have circumferential stress due to the internal pressure, but also because of their having curvature such that bulging arises around the crack. Folias analyzed stress intensity factors for thin-walled cylinders having cracks that pass through axially and discovered the theoretical relationship between the breaking stress for cylinders and the breaking stress for flat plates.[12), 13)]

$$\sigma^*_H = \sigma^* M^{-1} \qquad \text{(Eq. 10)}$$

$$M = \left[1 + 1.61\frac{C^2}{R_i \cdot t}\right]^{\frac{1}{2}} \qquad \text{(Eq. 11)}$$

Here, σ^*_H is the critical stress of a cylindrical vessel, σ^* the critical stress of a flat plate, C 1/2 of the length of the crack in the axial direction, R_i the inside radius and t the thickness. M is called the bulging factor or the Folias factor, and it is independent of the properties of the material. It is determined by the shape of the cylinder and of the crack. Folias found M by theoretical analysis based on stress intensity factor calculations, but Hahn has proposed basing critical stress that takes into consideration the plastic range on the M derived by Folias for applications in materials where the toughness is medium in degree or higher. The critical stress σ_f for cylinders of high toughness materials proposed by Hahn is expressed as follows using flow stress σ_{flow}.[14)]

$$\sigma_f = \sigma_{flow} M_t^{-1} \qquad \text{(Eq. 12)}$$

$$M_t = \left[1 + 1.61\frac{C^2}{R_i \cdot t}\right]^{\frac{1}{2}} \qquad \text{(Eq. 13)}$$

3. Critical Stress of Cylindrical Vessels Having Surface Cracks

In contrast to the critical stress for cylindrical vessels having cracks that pass through, the critical stress for cylindrical vessels having surface cracks is formulated using M_t in the analysis of cracks that pass through. As is shown in **Fig. 2**, there is a rectangular surface crack in the axial direction, and there are two types for the critical stress for a pressure cylinder that fractures

under conditions of large-scale yielding, a net section collapse equation and a local collapse equation.

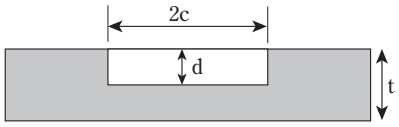

Fig. 2 Longitudinal crack-like flaw model

The critical stress σ_f^* is expressed by the following equation using the flow stress σ_{flow}.

$$\sigma_f^* = \sigma_{flow} M_s^{-1} \quad \text{(Eq. 14)}$$

M_s is a shape compensation factor for surface cracks, and it is expressed using M_t. The local collapse equation and net section collapse equation are as follows.[15)]

– Local collapse equation

$$M_s = \frac{1 - \frac{1}{M_t}(1 - R_t)}{R_t} \quad \text{(Eq. 15)}$$

– Net section collapse equation

$$M_s = \frac{1}{R_t + \frac{1}{M_t}(1 - R_t)} \quad \text{(Eq. 16)}$$

$$R_t = 1 - \frac{d}{t} \quad \text{(Eq. 17)}$$

Here, R_t is the remaining thickness ratio, d the crack depth and t the thickness. The main difference between the two is the behavior of M_s when $d \to t$. For M_s in the local collapse equation, we have $M_s \to \infty$ for $d \to t$, and the critical stress converges at 0. For M_s in the net section collapse equation, we have $M_s \to M_t$ for $d \to t$, and the critical stress converges at the breaking stress value for cracks that pass through. Surface cracks are thought to pass through the plate thickness and form a state where the crack passes through when the local collapse load is reached. When the net section collapse load is reached, the cylindrical vessel is thought to break in the axial direction.

4. Extension to Local Metal Loss Assessments

If we consider a metal loss shape such as that in **Fig. 3** to be a crack projected longitudinally in a local metal loss assessment, the calculations for critical stress basically do not change even if the crack is exchanged for metal loss. However, with cracks, we can make the distinction between [local collapse = passing through of surface cracks] and [net section collapse = axial failure of the vessel], but with metal loss, there is no concept of "progress of the crack," so this distinction cannot be made. In addition, handling metal loss which spreads out in three dimensions with the unaltered equation expressing the critical stress for cylindrical vessels with cracks does not always yield results close to reality. Therefore, we must find a factor corresponding to M_s in Eq. 14 to express the failure of cylindrical vessels with metal loss.

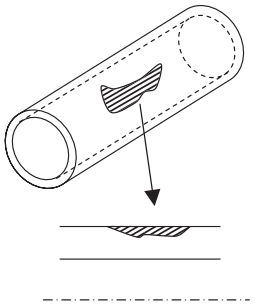

Fig. 3 Projection of Local Thin Area in cylindrical component

In API/ASME FFS-1, the failure mode is specified as plastic collapse, and the factor known as *RSF* is defined as a plastic collapse load ratio. The factor corresponding to M_s^{-1} corresponds to *RSF*.

In API/ASME FFS-1, a total of 32 types of evaluation equations are cited for determining the equation for calculating the *RSF* used in the standards, and investigations were made into a suitable method. The details of the investigation carried out for API/ASME FFS-1 are as follows.[16)]

(1) Burst tests and collection of the results of FEM analysis

Nearly 1000 burst tests accumulated by API/ASME and the results of FEM analysis were collected, and vessel shape, shape of metal loss and critical stress were put in order.

(2) Calculation of failure pressure

RSF was calculated by each of the 32 evaluation methods for each of the tests and analytical conditions (vessel shape and metal loss shape) that were both put in order in (1). Failure pressure is found using the following equation.

$$P_f = P_{fo} \times RSF \quad \text{(Eq. 18)}$$

Here, P_{fo} is the failure pressure of an undamaged component. For API/ASME FFS-1, an equation proposed by Svensson is used.

$$P_{UC} = \sigma_{uts}\left(\frac{e}{n}\right)^n\left(\frac{0.25}{n+0.227}\right)\cdot\ln\left[\frac{R_o}{R_i}\right] \quad \text{(Eq. 19)}$$

Here, n is the work hardening coefficient of the material.

(3) Comparison of burst test and FEM analysis results with failure pressure found from the formula for calculating *RSF*

We compared the tests and analytical results collected in (1) and the failure pressure calculated in (2).

As a result of investigating the equation that best matched the burst test results and analytical results from the 32 methods, the following equation was used for *RSF* (API/ASME FFS-1 Part 5 Level 1 Cylindrical Vessels).

$$RSF = \frac{R_t}{1-\frac{1}{M_t}(1-R_t)} \quad \text{(Eq. 20)}$$

Here, we have :

$$R_t = \frac{t_{mm}-FCA}{t_c} \quad \text{(Eq. 21)}$$

$$M_t = 1.0010 - 0.014195\lambda + 0.29090\lambda^2 - 0.096420\lambda^3 + 0.020890\lambda^4 - 0.0030540\lambda^5 + 2.9570(10^{-4})\lambda^6 - 1.8462(10^{-5})\lambda^7 + 7.1553(10^{-7})\lambda^8 - 1.5631(10^{-8})\lambda^9 + 1.4656(10^{-10})\lambda^{10} \quad \text{(Eq. 22)}$$

$$\lambda = \frac{1.285_S}{\sqrt{D_i\, t_c}} \quad \text{(Eq. 23)}$$

R_t : Remaining thickness ratio
t_{mm} : Minimum measured thickness
FCA : Future corrosion allowance
s : Length of metal loss in axial direction
t_c : Sound thickness at location away from part with metal loss
D_i : Inside diameter of vessel

Eq. 20 has the same shape as the inverse of the local collapse equation M_s for surface cracks. However, M_t was derived by finding the results of a last of elastoplasticity analysis using the finite element method (FEM) implemented by Jannele et al.

5. Evaluations of Bending Load (Axial Stress)

Up to this point we have given an overview of evaluation methods for equipment with internal pressure. On the other hand, it is also necessary to evaluate equipment with bending loads. Applications to equipment undergoing bending loads are impossible with Level 1 assessments in API/ASME FFS-1 Part 5. In Level 2 assessments, an evaluation formula using the modulus of section based on material dynamics is given for assessment of the effects of bending loads. This is assessed using the von Mises equivalent stress calculated from the axial stress due to circumferential stress caused by internal pressure, internal pressure, working load and seismic load.

In this article, we are omitting the details, but it is possible to carry out assessments of seismic load by carrying out API/ASME FFS-1 assessments related to bending load.

Burst Tests on Pipes with Metal Loss and FEM Simulations[17), 18)]

In the previous section, we explained the technical background of local metal loss assessments using API/ASME FFS-1 following the order of plastic collapse loads for sound cylindrical vessels. In API/ASME FFS-1, the formulae for computations were deep term and from distracted testing and the results of FEM simulations for extending crack assessments to local metal loss assessments. What is important in aiming to introduce Fitness-For-Service assessment technology to Japan can be thought of as being an accumulation of burst tests and FEM simulation results domestically and verification of the safety of international standards. In addition, these results will be effective for developing damage assessment methods in the future. In this article, we will introduce the burst test carried out by the authors to verify the safety margin in API/ASME FFS-1. In addition, we will also introduce the results of critical stress calculations using FEM simulations.

1. Verifications Based on Burst Tests in Pipes with Metal Loss

RSF calculations in API/ASME FFS-1 do not involve the length of metal loss in the circumferential direction. In other words, the critical stress for vessels where the width (length of metal loss in the circumfer-

ential direction) of the metal loss is narrow and the width of the metal loss is wide is the same if the length of the metal loss in the axial direction and the smallest measured thickness are the same. However, if the pressure in these cylindrical vessels with metal loss is added, it is presumed that the metal losses with narrow widths can be estimated from the deformation due to the effects of plastic constraints by the sound thick part of the periphery. Safety is verified using burst tests as opposed to evaluations where plastic collapse loads for metal loss with a narrow width and metal loss with a wide width are the same.

(1) Test conditions

For specimens, we used eight carbon steel pipes for machine structural use, JIS G3445STKM13A (outside diameter 150 mm, thickness 10 mm, length 1 m), and each of the test samples was locally turned on a lathe into one location in the middle of the outside surface to give it a part with metal loss (see **Fig. 4**). The details of the dimensions of the parts with metal loss are given in **Table 1**. Test piece No. 1 and test piece No. 5 are shown in **Fig. 5** as examples of the outside appearance of the specimens before the tests.

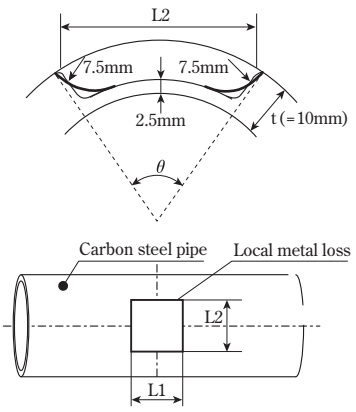

Fig. 4 Size of metal loss

Table 1 Size of local metal loss

Specimens No.	L1 (mm)	L2 (mm)	θ (°)
1	75	26	20
2	75	26	20
3	75	26	20
4	75	75	60
5	75	75	60
6	75	75	60
7	75	15	Groove
8	75	15	Groove

Fig. 5 Outer view of specimens

(2) Test Results

Test piece No. 1 and No. 5 are shown in **Fig. 6** as examples of the outside appearance after the tests. The test results are given in **Table 2**. Almost no difference was found in failure pressure, and the average failure pressure for the eight specimens was 36.0MPa.

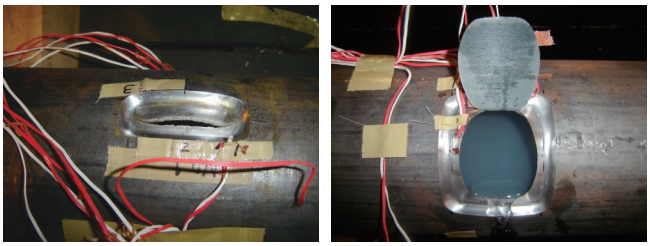

Specimen No.1 Specimen No.5

Fig. 6 Outer view of specimens after tests

Table 2 Test results

Specimens No.	Burst pressure (MPa)
1	35.8
2	40.2
3	34.9
4	36.3
5	32.1
6	37.6
7	36.1
8	35.2

These results agree with the concept in API/ASME FFS-1, in which the length of the metal loss in the circumferential direction does not contribute to the calculation of *RSF*.

(3) Comparison of $MAWP_r$ for pipes with metal loss and failure pressure

Next, we will evaluate $MAWP_r$, which is the maximum working pressure allowed by API/ASME FFS-1 for these pipes with metal loss, and confirm the safety margin by comparing this with the results of burst tests. In this article the safety margin S_M is defined as in the following equation.

$$S_M = \frac{F_{PM}}{MAWP_r} \quad \text{(Eq. 24)}$$

Here, F_{PM} is failure load due to the pressure and bending load.

First of all, we calculate $MAWP_r$ based on API/ASME FFS-1 from the conditions of the pipes with metal loss in the specimens. However, since STKM13A is carbon steel pipe for machine structural use, the allowable stress in the design criteria is not shown. Therefore, we decided to use the allowable stress (based on JIS B 8265) at normal temperatures for carbon steel pipes for high temperature pipes, JIS G3456STPT370, for which the specified minimum tensile strength is the same. There, the allowable stress for STPT370 at normal temperatures is 92MPa. $MAWP$ is found as follows from Eq. 5. Here, the weld joint efficiency is set to 1, the thickness t_c at the location away from the metal loss to 10 mm and FCA to 0 mm.

$$MAWP = \frac{92 \times 1 \times 10}{65 + 0.6 \times 10} = 12.96MPa \quad \text{(Eq. 25)}$$

Next, λ, M_t and RSF are calculated as follows from Eq. 23, Eq. 22 and Eq. 20 from the dimensions of the pipes with metal loss.

$$\lambda = 2.67 \quad \text{(Eq. 26)}$$

$$M_t = 1.94 \quad \text{(Eq. 27)}$$

$$RSF = 0.41 \quad \text{(Eq. 28)}$$

Since $RSF < 0.9$, $MAWP_r$ for the pipes with metal loss is as follows.

$$MAWP_r = MAWP\frac{RSF}{RSF_a} = 12.96 \times \frac{0.41}{0.9} = 5.90 \quad \text{(Eq. 29)}$$

While the $MAWP_r$ for the pipes with metal loss is 5.90MPa, the failure pressure according to the burst tests was an average of 36.0MPa, and the safety margin was 6.1. In the test conditions this time, the length of metal loss in the axial direction and the minimum measured thickness are the same, and even if the metal loss in the circumferential direction changes, it can be said to be a sufficient safety margin.

The cause of there being a large safety margin is that a sufficient design margin for the allowable stress was established as shown in **Fig. 1**. In addition, we can assume that the safety margin increased because of the following factors.

– Difference between minimum specified tensile strength and actual tensile strength

The minimum specified tensile strength is 370MPa, which is the same for STKM13A and STPT370. The tensile strength value for the carbon steel pipes used as specimens in this article was 451MPa. Therefore, the larger the difference between the minimum specified value and the actual value is, the greater the safety margin.

– Equation for calculating RSF

If the RSF calculation results shown by Eq. 28 are smaller than the actual remaining strength factor, the method according to API.ASME FFS-1 estimates on the conservative side. When the burst tests were conducted on pipes without metal loss using the same materials and same heat materials as the samples in this article, the failure pressure was 63.1MPa. If we think of the ratio of the failure pressure for the pipes with metal loss and the pipes without metal loss, RSF = 36.0 / 63.1 = 0.57. These calculation results for RSF were RSF = 0.41, and we can assume that the safety margin increased since it is a value that is more conservative than the actual one.

2. Calculation of failure pressure using FEM simulations

The failure pressure found with burst tests is calculated using FEM simulations. Failure pressure simulations with good precision will be effective in the future for accumulation of safety data.

Fracture criteria must be given to calculate failure pressure. In this article, we used the criteria proposed by Miyazaki.

(1) Analytical conditions

ANSYS 11.0 was used for the analysis solver. Analysis was carried out on three cases, a pipe with a narrow metal loss (θ = 20°) for Case 1, a pipe with a wide

metal loss (θ = 60°) for Case 2 and a pipe with a groove shaped metal loss for Case 3. The length of the metal loss in the axial direction was 75 mm for all of them, and the ligament thickness was 2.5 mm. Case 1 corresponds to burst test pieces No. 1 through 3, Case 2 to test pieces No. 4 through 6 and Case 3 to test pieces No. 7 through 8. As an example of the analytical model, **Fig. 7** shows the finite element model for Case 1.

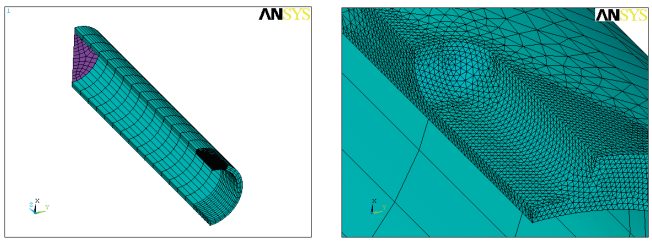

Fig. 7 Example of the finite element meshes (Case1, θ = 20°)

Test pieces were collected from parts of the pipes for which water pressure burst tests were carried out for the material characteristics, and the true stress-true strain relationship was obtained by carrying out tensile tests. In addition, the true fracture stress σ_{uf} and true fracture ductility ε_{uf} were as follows assuming fixed conditions for plastic volume and with the same aperture ϕ during fracture and aperture after fracture.

$$\sigma_{uf} = \sigma_f^{(n)} \frac{100}{100-\phi} \qquad \text{(Eq. 30)}$$

Here, $\sigma_f^{(n)}$ is the nominal stress during fracture.

$$\varepsilon_{uf} = \ln\left(\frac{A_o}{A}\right) = \ln\left(\frac{100}{100-\phi}\right) \qquad \text{(Eq. 31)}$$

Since the nominal stress during fracture of the pipe was 315.4MPa and the aperture was 68%, the true fracture stress σ_{uf} and true fracture ductility ε_{uf} were

σ_{uf} = and 986MPa, ε_{uf} = 1.14.

A poly-linear approximation was carried out from a true stress-true strain diagram obtained from the nominal stress-nominal strain diagram and the true breaking stress σ_{uf} and true fracture ductility ε_{uf} obtained from the aperture after the tensile tests, and the material model shown in **Fig. 8** was obtained.

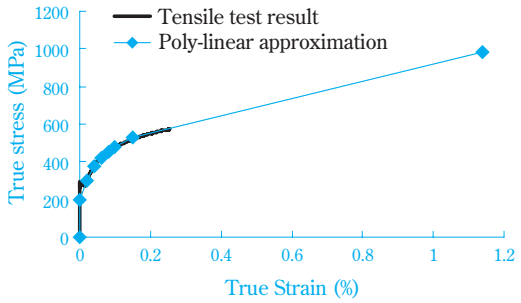

Fig. 8 Stress-strain curve for FEA

(2) Strain calculation results

The stress and strain were calculated at various locations when the analytical conditions shown in (1) were increased. In the burst tests for Case 1 and Case 2, strain was measured by the gain in strain, and the test results and simulation results were compared. The results of comparing the burst tests and the simulations for the changes in strain at the center of the metal loss are shown in **Fig. 9**. The two agree well, and we can assume that the simulation results were able to reproduce the actual behavior. The cause of this is thought to be that the material characteristics for the true stress-true strain relationship given to the simulation agree well with the actual ones.

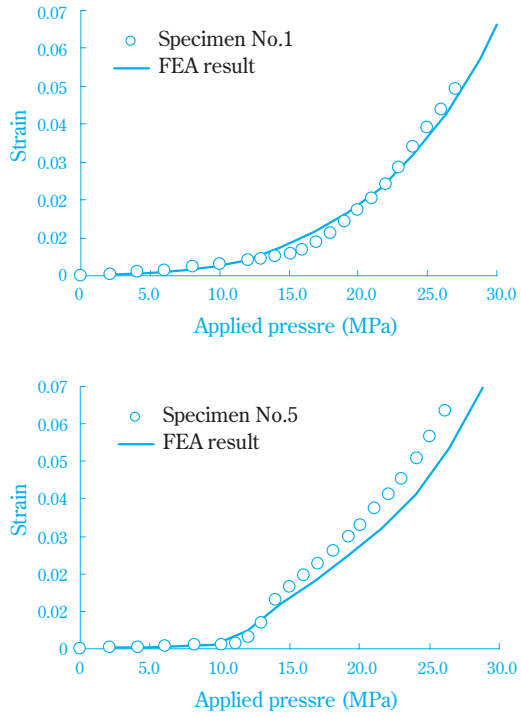

Fig. 9 Relationship between applied pressure and strain of specimens

(3) Fracture criteria

The true fracture ductility in a multiaxial stress field is lower than the true fracture ductility obtained from tensile tests having monoaxial stress field conditions. For the criteria for multiaxial stress fields, Miyazaki et al. have extended the isostatic pressure breaking criteria of Weiss, in which breaking arose when the isostatic pressure reached a critical static water pressure.[19)]

Miyazaki et al. have said that the following equation arises for the true fracture ductility ε_{mf} and the true fracture stress σ_{msf} in multiaxial strain conditions when the stress and strain relationship is expressed by a Ramberg-Osgood approximation.

$$\left(\frac{\varepsilon_{mf}}{\varepsilon_o}\right)=\left(\frac{\sigma_{msf}}{\sigma_o}\right)+a\left(\frac{\sigma_{msf}}{\sigma_o}\right)^n \qquad \text{(Eq. 32)}$$

$\sigma_o = \sigma_y$: yield stress, $\varepsilon_o = \sigma_o/E$, E: modulus of elasticity, a: material constant, n: material constant

In addition, the true fracture ductility ε_{mf} in a multiaxial strain field is formulated as follows.

$$\varepsilon_{mf}=\frac{\left(\frac{\omega m\sigma_{uf}}{\sigma_o}\right)+a\left(\frac{\omega m\sigma_{uf}}{\sigma_o}\right)^n}{\left(\frac{\sigma_{uf}}{\sigma_o}\right)+a\left(\frac{\sigma_{uf}}{\sigma_o}\right)^n}+\varepsilon_{uf} \qquad \text{(Eq. 33)}$$

Here, ω and m are as follows.

$$\omega=\frac{1}{1+\alpha+\beta} \qquad \text{(Eq. 34)}$$

$$m=\sqrt{(1+\alpha+\beta)^2-3(\alpha+\beta+\alpha\beta)} \qquad \text{(Eq. 35)}$$

$\alpha = \sigma_2/\sigma_1$, $\beta = \sigma_3/\sigma_1$: σ_1 first principal stress, σ_2 second principal stress, σ_3 third principal stress

Here, the true fracture ductility in Eq. 33 was used as the failure condition. Specifically, ω and m were calculated from the stress distribution for each pressure found by the FEM analysis and the true fracture ductility found. A comparison was made with the corresponding strain at that location, and a determination on breaking was made. In addition, in terms of the material constants a and n, a = 16.9 and n = 3.1 from the material characteristics in **Fig. 8**.

(4) Results of failure pressure simulations

The relationship between the true fracture ductility and the equivalent strain at the location where stress and maximum strain occur is shown in **Fig. 10**. When the stress increases the equivalent strain also increases, and fracture is thought to occur when it crosses the line of the true fracture ductility. **Table 3** gives the results of finding the breaking stress in each case from **Fig. 10**.

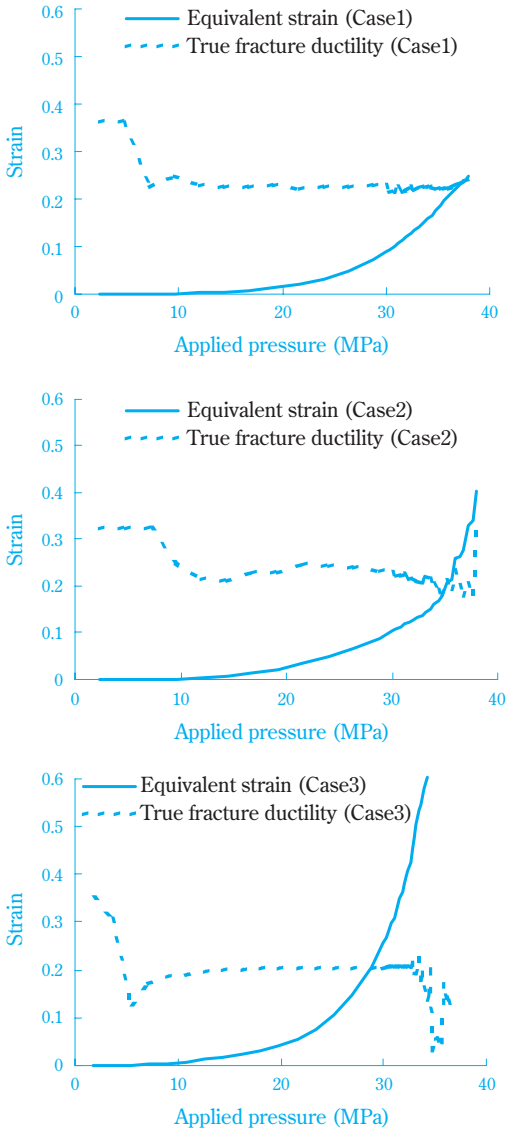

Fig. 10 Estimation for burst pressure for cylindrical vessel

Table 3 Simulation results

Case No.	Burst pressure (MPa)
1	36.8
2	35.2
3	28.8

Comparing this with the results of the burst tests (average of six pipes being 36.0MPa), the results of the Case 1 and Case 2 simulations match the actual tests well. For the groove shaped metal loss in Case 3, the

simulation results were 28.8MPa, which were results more on the conservative side than the actual test results. The cause of this is thought to be the poly-linear approximation being affected by possibilities different from the actual ones and the processing precision of the groove shaped metal loss in the sample material (dimensions and surface state).

As in the above, a result on the conservative side of the actual appeared for the groove shaped metal loss, but it showed that it is possible on the whole to calculate the actual breaking stress by FEM simulations. Moving forward, we can expect that safety data can be accumulated by this same method.

Investigations by the Petroleum Association of Japan and the Japan Petrochemical Industry Association

The Fitness for Service Study Group of the Petroleum Association of Japan and the Japan Petrochemical Industry Association is carrying out surveys and investigations on fitness for service assessments mainly for local metal loss.[9), 20), 21)] This study group was established in 1999 and carried out the investigations of the details of the draft version of API RP579, which was the predecessor of API/ASME FFS-1. The beginning of activities was reflecting Japanese opinions in the first version of API RP579.

After that, an official committee member was sent for API TG579, and this member has participated in the deliberations on proposed revisions and voting ballots since 2002. This contributed to the issuing of API/ASMEFFS-1 which is the joint standard of the ASME and API being brought up in this article. Here, we will introduce some of the results of investigations being carried out by this study group.

1. Results of Burst Tests in Japan and Comparison with Assessment Results for API/ASME FFS-1[22)]

To move forward in the verification of API/ASME FFS-1, results where the test load is not only internal pressure but also includes bending loads are necessary. The FFS study group has collected breaking test data on cylindrical vessels to which internal pressure loads, bending loads and composite inside pressure and bending loads have been applied and has investigated the safety margins of API/ASME FFS-1. The results are shown in **Fig. 11**. Here, the total for the number of data is 49, and (1) in the figure is High Pressure Gas Safety Institute of Japan data from 1998, (2) High Pressure Gas Safety Institute of Japan data from 1990, (3) Osaka High Pressure Gas Safety Institute data from 1992, (4) JFE engineering test data and (5) data from 2006 the Ibaraki Prefecture High Pressure Gas Facility Maintenance Criteria Formulation Program.

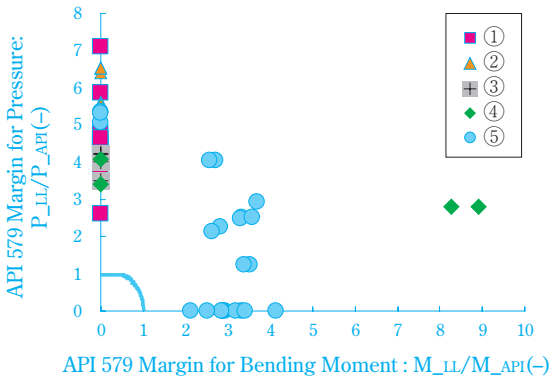

Fig. 11 Safety margin of API/ASME FFS-1 Part 5

The horizontal axis is the safety margin for the bending moment, and the vertical axis is the safety margin for the internal pressure. It can be seen that for the bending moment as well as for the internal pressure, the safety margin versus the burst tests is 2 or greater. This shows that a sufficient safety margin may be maintained in various load conditions.

2. Collection of Test Data on the High Temperature Range in Carbon Steel

The difference between a minimum specified strength and actual tensile strength have been cited as having an effect on the safety margin. The FFS Study Group has carried out verifications of the tensile strength for typical carbon steels. In addition, since burst tests are difficult to carry out at high temperatures, tensile tests were carried out at various temperatures from normal temperatures to 300°C for the purpose of confirming safety up to approximately 300°C. Part of the results is shown in **Fig. 12** and **Table 4**.

Fig. 12 is an investigation of the stress-strain curves from normal temperatures to 300°C for SM490A. It shows that there is sufficient margin in all temperature ranges for a minimum specified tensile strength of 490MPa. In addition, the behavior of the stress-strain

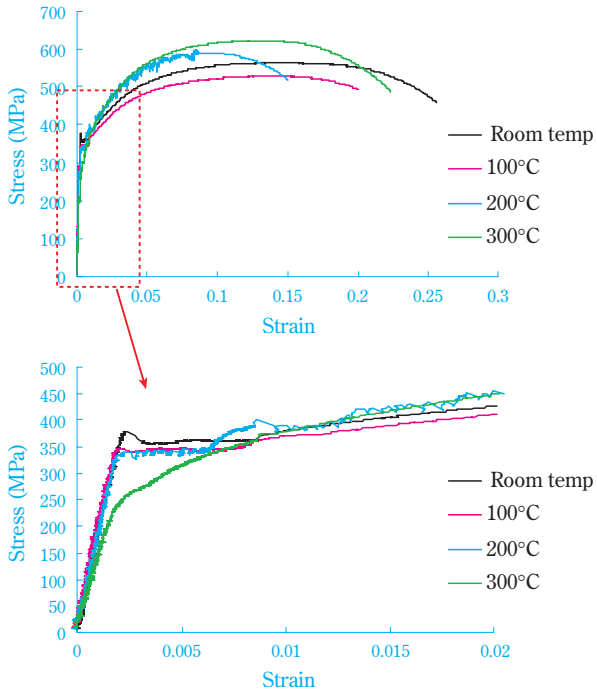

Fig. 12 Results of tensile test of SM490A

Table 4 Results of tensile test of SM490A

Room temp	
Tensile strength	561MPa
Yield stress	355MPa
100°C	
Tensile strength	525MPa
Yield stress	343MPa
200°C	
Tensile strength	597MPa
Yield stress	337MPa
300°C	
Tensile strength	621MPa
Yield stress (at 0.2%)	300MPa

curve in the neighborhood of yield stress is substantially the same behavior from normal temperatures to 200°C, and even though no clear yield stress is exhibited at 300°C, there is a blue brittleness effect, and the tensile strength is the greatest at 300°C.

From the results of the tensile tests as well, the actual tensile strength is higher than the minimum specified tensile strength, so even with *RSF* = 0.9, which is the basic concept of API/ASMEFFS-1, it can be assumed that there is a sufficient safety margin.

Conclusion

Recently, the safety inspections in the High Pressure Gas Safety Act have moved to specific safety guidelines for safety assurance of pressure equipment in domestic plants, and the detailed specifications are to be transferred to consumer specifications.

While freedom for inspections will increase, the responsibility of businesses like us to carry out our own inspections will increase. Within this, it is necessary to have cooperation among industry, academia and government and obtain a consensus for incorporating new technology and international standards and establishing self-imposed inspections that are compatible with societal requirements (safety, economy and internationalism). The role of those of us in industry may be thought of as getting a grasp on and understanding the trends in international standards and continuously accumulating safety data. In particular, with the globalization of economic activities, it is extremely important for international standards and domestic standards to agree. In this article, we have given an overview of the content of API/ASME FFS-1 local metal loss assessments and shown safety data. The application of these evaluation methods to pressure equipment under the Gas Business Act has already been approved. We are also aiming at introduction of self-imposed inspection methods based on international standards in other pressure equipment, and we will continue to get an understanding of the technology and accumulate data.

Acknowledgments

During this research we received a large amount of guidance and advice from the members and technical advisers of the Fitness for Service Study Group of the Petroleum Association of Japan and the Japan Petrochemical Industry Association. We would like to take this opportunity to express our deep gratitude to them.

References

1) JIS B8265 Construction of pressure vessel –General principles, **2003**.
2) ASME Boiler and Pressure Vessel Code Section VIII Division 1, **2007**.
3) H. Kobayashi, *Journal of the Japanese Society for Non-Destructive Inspection*, **52**(5), 229(2003).
4) JSME S NA1 Code for Nuclear Power Generation Facilities –Rules on Fitness-for-Service for Nuclear Power Plants–, **2004**.
5) API 579-1/ASME FFS-1 Fitness-For-Service, **2007**.

6) H. Kobayashi, *Journal of the Society of Materials Science, Japan*, **56**(5), 483(2007).
7) JIS B8266 Alternative standard for construction of pressure vessels, **2003**.
8) JIS B8267 Construction of pressure vessel, **2008**.
9) I. Kozima, T. Kikuchi, T. Tahara, *Journal of High Pressure Institute of Japan*, **44**(4), 18(2006).
10) T. Kaida, *Proceedings of JHPI autumn conference 2006*, 28(2006).
11) S. Machida, "Ensei Hakai Rikigaku (Ductile Fracture Mechanics)", Nikkan Kogyo Shimbun Ltd. (1984), p.189.
12) E.S. Folias, *International Journal of Fracture Mechanics*, **1**, 20(1965).
13) E.S. Folias, *International Journal of Pressure Vessels and Piping*, **76**, 803(1999).
14) G.T. Hahn, M. Sarrate, A.R. Rosenfield, *International Journal of Fracture Mechanics*, **5**(3), 187(1969).
15) G.G. Chell, TPRD/L/MT0237/M84, ADISC, ADISC, **1984**.
16) J.L. Janelle, D.A. Osage, S.J. Burkhart, WRC Bulletin 505, **2005**.
17) T. Kaida, ASME PVP2008-61806, **2008**.
18) T. Kaida, *Proceedings of JHPI autumn conference 2007*, 44(2007).
19) K. Miyazaki, A. Nebu, S. Kanno, M. Ishiwata, K. Hasegawa, *Journal of High Pressure Institute of Japan*, **40**(2), 62(2002).
20) Y. Ideguchi, Y. Ishizaki, T. Tahara, *Journal of High Pressure Institute of Japan*, **44**(5), 25(2006).
21) A. Ohno, Y. Uno, T. Tahara, *Journal of High Pressure Institute of Japan*, **44**(6), 27(2006).
22) A. Ohno, T. Tahara, ASME PVP2008-61845, **2008**.

PROFILE

Takuyo KAIDA
Sumitomo Chemical Co., Ltd.
Process & Production Technology Center